Internal stress in kinetically trapped actin bundle networks†

Kurt M. Schmoller, Oliver Lieleg and Andreas R. Bausch*

Received 21st May 2008, Accepted 8th September 2008
First published as an Advance Article on the web 23rd September 2008
DOI: 10.1039/b808582j

By confocal microscopy combined with local cutting of single bundles, we show that the actin binding protein filamin is already sufficient to generate prestress in *in vitro* actin networks by cross-linking and bundling actin filaments during network polymerization forming a kinetically trapped network structure.

Introduction

One of the main characteristics of living organisms is the power to adapt to as well as generate environmental changes. Cells are able to exert forces not only on their environment but also exhibit internal forces which correlate with the cellular elasticity[1] resulting in an extremely high adaptability of cell stiffness. So far it is assumed that in cytoskeletal actin networks stabilizing internal prestress is generated either actively by molecular motors like myosin or passively by tension caused by the surrounding extracellular matrix[1,2]—both suggesting internal stress to be a non-equilibrium effect. *In vitro* experiments, where both physical and chemical parameters can be controlled may turn out to be useful for a profound understanding of the underlying physical principles that lead to prestressed networks of semi-flexible polymers.[3] *In vitro* reconstitutions of cytoskeletal actin networks exhibiting internal stress by molecular motors have already been established.[4] However, *in vitro* actin networks lacking active molecular motor activity have so far been expected to be sufficiently thermally equilibrated to legitimate the applicability of theoretical equilibrium models.[3]

Here, we show that surprisingly the cross-linking molecule filamin alone is sufficient to generate prestress in *in vitro* actin networks. We demonstrate that filamin creates bundled actin networks, which are kinetically trapped and exhibit internal stresses.

Materials and methods

G-actin was obtained from rabbit skeletal muscle and prepared as described before.[5] Muscle filamin was isolated from chicken gizzard and further purified as reported in ref. 6. Polymerization was initiated in the presence of filamin by adding 1/10 volume of 10 × F-buffer (20 mM Tris, 20 mM $MgCl_2$, 2 mM $CaCl_2$, 1 M KCl and 2 mM DTT, pH 7.5) and gently mixing for 10 s. Afterwards the sample was immediately loaded into a flow chamber.

Confocal images were taken with a confocal Leica TCS SP5 microscope. Images shown here are projections of a confocal image stack, in which images are equally distributed over a height of 30 μm to 40 μm. To investigate the network polymerization actin was labelled and stabilized with phalloidin-TRITC (Sigma). In the photobleaching experiments actin was labelled with either phalloidin-TRITC or Alexa Fluor 555 (Invitrogen) without any effect on the experimental outcome. In order to locally disintegrate the network a distinct small sample volume was excited with the highest laser intensity available. This excitation was maintained for a few seconds for Alexa Fluor 555 labelled actin and for a few minutes for phalloidin-TRITC labelled—and thus stabilized—actin.

Results and discussion

Filamin is known to cross-link actin filaments at low molar ratios whereas at high concentrations a bundle network is formed.[7] In contrast to other actin binding proteins (ABPs) which—like fascin—

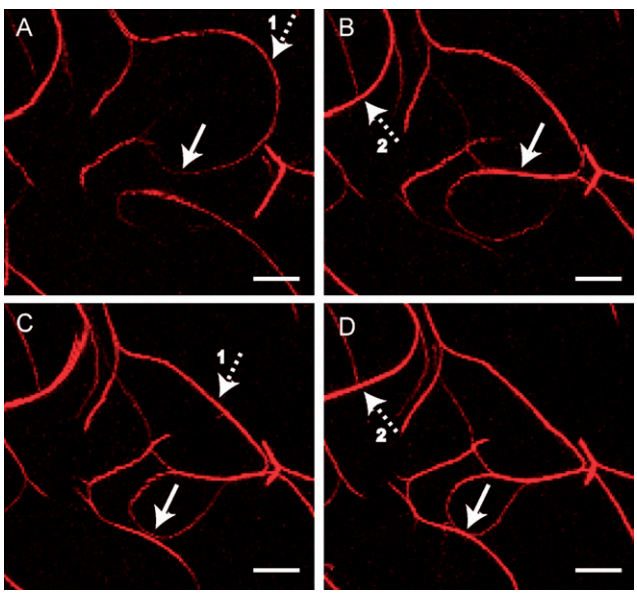

Fig. 1 Confocal images (*z*-projection of a 40 μm stack) of a phalloidin-TRITC labelled actin network (2.4 μM) bundled by filamin (0.24 μM): images are taken about 8 (A), 10 (B), 13 (C) and 17 (D) min after polymerization was initiated. Closed arrows denote where branches are formed (one from A to B, one from C to D). The network is deformed due to internal forces resulting from the continuous polymerization of filaments. Dashed arrows denote bundles with changing curvature (1 change from A to C, 2 changes from B to D). Scale bars denote 10 μm.

E27 Lehrstuhl für Biophysik, Technische Universität München, James-Franck-Str, 85747 Garching, Germany. E-mail: abausch@ph.tum.de; Fax: + 0049 89 289-12469; Tel: + 089 289-12480

† Electronic supplementary information (ESI) available: Video 1: polymerization of actin (2.4 μM) in the presence of filamin (0.24 μM), video 2: the image sequence corresponding to Fig. 2, video 3: confocal images (*z*-projection of a 60 μm stack) of an actin network (2.4 μM) bundled by filamin (0.48 μM) before and after local photobleaching and Fig. S1: overlay of the two confocal images shown in video 3. See DOI: 10.1039/b808582j

form straight, cross-linked actin bundles,[8] actin–filamin bundles are highly curved and form branches (Fig. 1).

In order to determine the origin of these branched structures the polymerization of actin–filamin networks is investigated with confocal microscopy: the polymerization process is observed to be accompanied by a continuous, highly dynamic reorganization of previously formed bundle structures. Strikingly, the formation of new branches is detectable: bundles which come into close proximity by thermal excitation or network deformations fuse—beginning at the first point of encounter. Further merging of the bundles results in a clear deformation of the surrounding network, which includes drastic changes of the bundle curvatures and therefore leads to local build-up of internal stress (Fig. 1 and ESI†).

These deformations give rise to further reorganization events in the network as new connections between bundles are formed. Therefore, the build-up of internal strain has an almost autocatalytic character: local deformations provide the basis for new bundle branches, which in turn give rise to further long range deformations inside the network. The interaction range is set by the persistence length of the bundles, which therefore determines not only the mechanical response of the equilibrated bundle network but also its dynamic construction.

After ~1 h the network formation is finished and a highly static and stable structure emerges. Hardly any changes are observable within days and no thermal excitations of the bundles are resolvable.

The speed of actin polymerization depends on the $MgCl_2$ concentration.[9] In order to slow down the polymerization and the concomitant reorganization process, an actin–filamin network is polymerized in F-buffer without $MgCl_2$. Under these conditions the formation of the network takes about 6 h. Bundle deformations and spontaneous network reorganizations are observed throughout the whole time period. The final network structure is almost indistinguishable from the respective control network in the presence of $MgCl_2$. This demonstrates that the filament polymerization is the critical step leading to the observed deformations and branch formations. Slowing down of the network polymerization by a factor of 9 does not result in different network structures. In contrast, by changing the order of the network formation, completely different network structures can be reached: adding filamin to already polymerized actin by diffusive mixing results in highly inhomogeneous networks mainly located in the area where the actin solution has come into contact with filamin (Fig. 2A). If filamin is added by manual mixing using a pipette, a high number of bundle clusters can be observed, which are not present if actin is polymerized in the presence of filamin (Fig. 2B). As the resulting networks are stable for days, this history dependence of the network structures provides additional evidence for the existence of kinetically trapped network structures.

To directly demonstrate the existence of internal stresses in actin–filamin bundle networks even in the static state, individual bundles are locally disintegrated by photobleaching. Upon successfully cutting an individual bundle a spontaneous and inhomogeneous reorganization of the surrounding network is observed (Fig. 3 and ESI†). Further network relaxation takes place during the following minute.

Similar effects are also observable at higher actin concentrations (up to 4.8 μM), although the decreased mesh size inhibits a controlled cutting of individual bundles (ESI†). Instead, destruction of a local part of the network leads to a more global relaxation of the surrounding network.

In summary, the network formation results in a kinetically trapped network structure where internal stresses are present: the local network structure, including the amount of internal stresses—and thus the local conformational energy—depends on distinct connection events occurring during polymerization. To further explore the energy landscape in order to find the total energy minimum, additional network reorganization would be needed—*e.g.* by unbinding and rebinding events between distinct bundles. The dissociation constant $K_D = 0.46$ μM and the off rate $k_{-1} = 0.6\ s^{-1}$ of actin and filamin[10] are comparable in magnitude to other ABPs, *e.g.* fascin.[11,12]

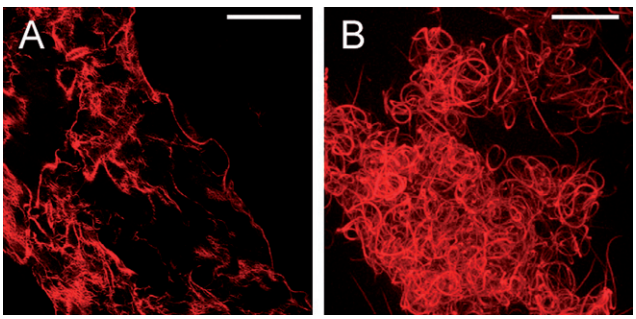

Fig. 2 (A): Filamin is added to actin (2.4 μM), which has already been polymerized in a flow chamber. Mixing of actin and filamin by diffusion results in an extremely inhomogeneous structure mainly located in the area where the actin solution has come into contact with the filamin solution. Scale bar denotes 100 μm. (B): Filamin (0.3 μM) is added to F-actin (3 μM) by manual mixing using a pipette. In contrast to the homogeneous network formed if actin is polymerized in the presence of filamin, a heterogeneous network with a high number of bundle clusters emerges. The confocal image (*z*-projection of a 60 μm stack) shows a characteristic cluster. Scale bar denotes 25 μm.

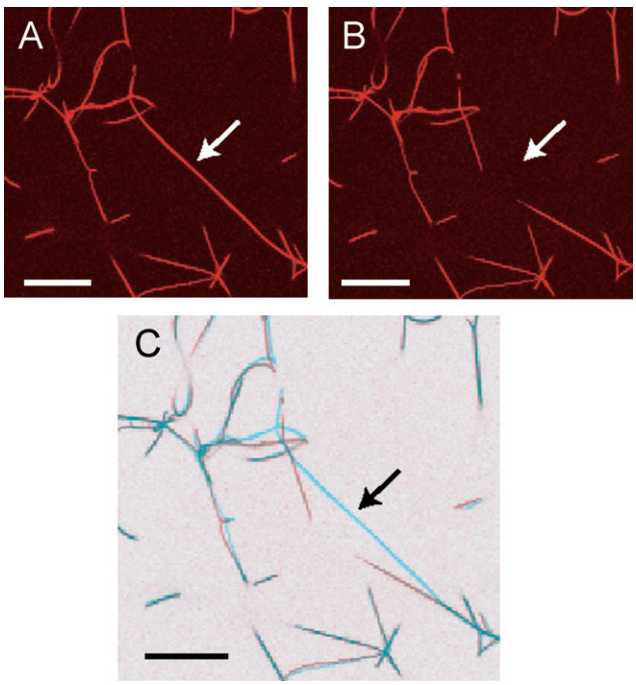

Fig. 3 Confocal images (*z*-projection of a 30 μm stack) of an actin network (0.95 μM) bundled by filamin (0.32 μM) before (A) and after (B) cutting one bundle by photobleaching. (C) shows an overlay of A (blue) and B (red). The arrow denotes the center of photobleaching. The network relaxes due to internal forces upon cutting the central bundle. Scale bars denote 50 μm.

However, in actin–fascin bundle networks a single unbinding event of a transient cross-linker suffices to allow local reorganizations.[13] In contrast, as actin–filamin bundles are highly branched and merged, multiple unbinding events have to occur in a concerted way to separate merged bundles and allow for further relaxation of actin–filamin networks. Thus, the timescale at which the network can reach full thermal equilibrium is not accessible. Furthermore, the branched network structure seems to be responsible for the observed extreme mechanical stability and strain hardening behavior. In turn, it is the molecular structure of filamin which is responsible for the branching.

While until now most *in vitro* reconstituted cross-linked actin networks were considered to be in thermal equilibrium, our results show that this must not necessarily be the case. Prestressing such networks may provide an important tool for cells to exert and withstand the forces occurring in cell migration or cell division. As the observed structures result in extremely well-repeatable mechanical properties, they are trapped in a very well-defined metastable state. This probably results from a highly balanced control of bundle mechanics, microscopic bundle structure and the build-up of internal stresses. Further studies have to address the mechanism of kinetically trapped semi-flexible polymer network formation and their functional role.

Acknowledgements

We thank C. Semmrich for helpful discussions and M. Rusp for protein preparation. This work was supported by Deutsche Forschungsgemeinschaft through Ba2029/8-1 and the DFG-Cluster of Excellence Nanosystems Initiative Munich (NIM). O. Lieleg acknowledges support from CompInt in the framework of the ENB Bayern.

Notes and references

1 N. Wang, I. M. Tolic-Norrelykke, J. Chen, S. M. Mijailovich, J. P. Butler, J. J. Fredberg and D. Stamenovic, *Am. J. Physiol.: Cell. Physiol.*, 2002, **282**, C606–C616.
2 S. Kumar, I. Z. Maxwell, A. Heisterkamp, T. R. Polte, T. P. Lele, M. Salanga, E. Mazur and D. E. Ingber, *Biophys. J.*, 2006, **90**, 3762–3773.
3 A. R. Bausch and K. Kroy, *Nat. Phys.*, 2006, **2**, 231–238.
4 P. M. Bendix, G. H. Koenderink, D. Cuvelier, Z. Dogic, B. N. Koeleman, W. M. Brieher, C. M. Field, L. Mahadevan and D. A. Weitz, *Biophys. J.*, 2008, **94**, 3126–3136.
5 Y. Luan, O. Lieleg, B. Wagner and A. Bausch, *Biophys. J.*, 2008, **94**, 688–693.
6 Y. Shizuta, H. Shizuta, M. Gallo, P. Davies and I. Pastan, *J. Biol. Chem.*, 1976, **251**(21), 6562–6567.
7 Y. Tseng, K. M. An, O. Esue and D. Wirtz, *J. Biol. Chem.*, 2004, **279**(3), 1819–1826.
8 O. Lieleg, M. M. A. E. Claessens, C. Heussinger, E. Frey and A. R. Bausch, *Phys. Rev. Lett.*, 2007, **99**, 088102.
9 C. T. Zimmerle and C. Frieden, *Biochemistry*, 1986, **25**, 6432–6438.
10 W. H. Goldmann and G. Isenberg, *FEBS Lett.*, 1993, **336**, 408–410.
11 S. Ono, Y. Yamakita, S. Yamashiro, P. T. Matsudaira, J. R. Gnarra, T. Obinata and F. Matsumura, *J. Biol. Chem.*, 1997, **272**, 2527.
12 Y. S. Aratyn, T. E. Schaus, E. W. Taylor and G. G. Borisy, *Mol. Biol. Cell*, 2007, **18**, 3928–3940.
13 O. Lieleg and A. R. Bausch, *Phys. Rev. Lett.*, 2007, **99**, 158105.